Satellite-based estimates of surface water dynamics in the Congo River Basin

M. Becker[1,*], F. Papa[2,3], F. Frappart[2,4], D. Alsdorf[5], S. Calmant[2], J. Santos da Silva[6], C. Prigent[7] and F. Seyler[8]

[1] LIENSs/CNRS, UMR 7266, ULR/CNRS, 2 rue Olympe de Gouges, La Rochelle, France

[2] LEGOS/IRD, UMR 5566, CNES/CNRS/IRD/UPS, 14 Avenue Edouard Belin, Toulouse, France

[3] Indo-French Cell for Water Sciences, IRD-IISc-NIO-IITM, Indian Institute of Science, Bangalore, India

[4] GET/GRGS, UMR 5563, CNRS/IRD/UPS, OMP, 14 Avenue Edouard Belin, Toulouse, France

[5] Byrd Polar and Climate Research Center and School of Earth Sciences, Ohio State University, OH, USA.

[6] UEA/CESTU, Av. Djalma Batista 3578, Manaus, Brazil

[7] CNRS, LERMA, Observatoire de Paris, Paris, France

[8] ESPACE-DEV/IRD, UMR 228, IRD/UM/UG/UR, MTD 500 rue J-F Breton, Montpellier, France

* *Corresponding author: melanie.becker@univ-lr.fr.*

Abstract

In the Congo River Basin (CRB), due to the lack of contemporary in situ observations, there is a limited understanding of the large-scale variability of its present-day hydrologic components and their link with climate. In this context, remote sensing observations provide a unique opportunity to better characterize those dynamics. Analyzing the Global Inundation Extent Multi-Satellite (GIEMS) time series, we first show that surface water extent (SWE) exhibits marked seasonal patterns, well distributed along the major rivers and their tributaries, and with two annual maxima located: i) in the lakes region of the Lwalaba sub-basin and ii) in the “Cuvette Centrale”, including Tumba and Mai-Ndombe Lakes. At an interannual time scale, we show that SWE variability is influenced by ENSO and the Indian Ocean dipole events. We then estimate water level maps and surface water storage (SWS) in floodplains, lakes, rivers and wetlands of the CRB, over the period 2003-2007, using a multi-satellite approach, which combines the GIEMS dataset with the water level measurements derived from the ENVISAT altimeter heights. The mean annual

variation in SWS in the CRB is 81±24 km^3 and contributes to 19±5 % of the annual variations of GRACE-derived terrestrial water storage (33±7 % in the Middle Congo). It represents also ~6±2 % of the annual water volume that flows from the Congo River into the Atlantic Ocean.

Keywords: Surface water storage; Congo River Basin; Remote sensing.

1. Introduction

Despite its importance, the Congo River Basin (CRB), located in the central region of Africa, has not attracted as much attention among the climate and hydrology communities as has the Amazon Basin or other large rivers in the world [*Alsdorf et al.*, 2016]. Up to now, there is still an insufficient knowledge of the regional hydro-climatic characteristics and changes in this region, even though the CRB plays a crucial role at global and regional scales. Firstly, the CRB is remarkable as the second largest river system of the world in terms of both water discharge, with a mean annual flow of ~40,600 m^3/s, and drainage basin size (~3.7×10^6 km^2) [*Laraque et al.*, 2001, 2009]. It also plays a key role in the Earth system as one of the three main convective centers in the Tropics, with the Amazon River basin and the 'maritime continent' of Eastern Indian and western tropical Pacific Oceans [*Hastenrath*, 1985]. Secondly, more than 80% of people in the CRB live exclusively on activities that are highly dependent on climate and water resource availability: fisheries, agriculture and livestock [*Bele et al.*, 2010]. In this region, the food production depends heavily on rain-fed agriculture, leading the population particularly vulnerable to food insecurity [*Brown et al.*, 2014]. Moreover, a couple of studies have shown that the CRB has already experienced changes in climate variability and in the hydrological system [*Mahé and Olivry*, 1999; *Camberlin et al.*, 2001; *Laraque et al.*, 2001; *Samba et al.*, 2008; *Samba and Nganga*, 2012]. Thirdly, about 50% of the CRB land area is covered by tropical forest (~190 10^6 ha, *Verhegghen et al.*, 2012), representing about

18% of the world's tropical forests (~1100 10^6 ha, *Achard et al.*, 2002), and playing a crucial role as a sink of CO_2, storing about 50 billion tons of carbon [*Verhegghen et al.*, 2012]. In a recent study, *Dargie et al.*, [2017] highlighted that the "Cuvette Centrale" peatland (Fig.1) stores about 30 billion tons of carbon. This total amount of carbon is equivalent to ~ 80 billion tons of CO_2 or about 2.3 years of current global anthropogenic emissions (~ 35 billion tons in 2015, *Olivier et al.*, 2016). This stock is particularly vulnerable to land-use change and any future change in the water cycle. For all these reasons, there is an obvious need to better understand the CRB dynamic and to characterize its vulnerability to climate change and other crucial challenges. In particular, it is necessary to gain solid knowledge about the past and current hydro-climate processes of the CRB, in order to significantly reduce the uncertainties associated with future climate response under global warming. The limited understanding of the CRB's hydro-climate processes results mainly from the lack of *in situ* data availability: the network of stations, which data are publicly released, is sparse and poorly maintained, and it is substantially difficult of perform fieldwork, notably in the swamps. However, recent developments and improvements in remote sensing technology provide more observations than ever before [*Alsdorf et al.*, 2007; *Prigent et al.*, 2016] and allow us the unique opportunity to better understand the spatial and temporal variability of the CRB's hydro-climatic patterns.

In this study, our primary focus is on the CRB surface water (SW) dynamics, a key component of the land water budget equation. The SW, corresponding to water stored in rivers, lakes, wetlands, floodplains and in man-made reservoirs, is crucial to the survival of all living organisms, including humans and is a precious resource in term of biodiversity, ecology, water management and economy. Moreover, SW storage (SWS) plays a major role at all scales in the terrestrial water balance and in the Earth's climate system variability, through its interactions with the atmosphere and ocean. Up until now, the spatial and temporal dynamics of SW stored on the Earth's surface remains still largely unknown [*Alsdorf et al.*, 2007]. Since the last decades, progresses in satellite remote sensing are improving substantially our understanding of SW dynamics in the major river basins of the world. Among these derived-products, radar altimetry is providing since the early 1990s a monitoring of water levels variations of lakes, rivers, floodplains and reservoirs [*Birkett*, 1995; *Crétaux and Birkett*, 2006; *Calmant et al.*, 2008]. Additionally, it is possible to extract locally the extent of water bodies using satellite imagery, which, combined with altimetry data, enable the SWS estimation of lakes and reservoirs [*Baup et al.*, 2014; *Crétaux et al.*, 2016] and of floodplains [*Frappart et al.*, 2005]. More recently, merging information derived from active and passive microwave sensors and from optical data, the Global Inundation Extent from Multi-Satellite (GIEMS) dataset [*Prigent et al.*, 2007; *Papa et al.*, 2010; *Prigent et al.*, 2016] offers unprecedented information on the variations of SW extent (SWE) at the global scale. The combination of GIEMS estimates with radar altimetry observations has further allowed the provision of spatio-temporal variations of SWS in large tropical river basins, such as the Amazon, Ganges–Brahmaputra and Orinoco basins [*Frappart et al.*, 2008, 2010, 2012, 2015b; *Papa et al.*, 2015]. Recently, a few studies tried to understand the SW dynamics in the CRB using remote sensing and/or modeling [*Rosenqvist and Birkett*, 2002; *Bwangoy et al.*, 2010; *Jung et al.*, 2010; *Beighley et al.*, 2011; *Lee et al.*, 2011; *Tshimanga et al.*, 2011; *Tshimanga and Hughes*, 2012; *O'Loughlin et al.*, 2013; *Becker et al.*, 2014; *Betbeder et al.*, 2014; *Lee et al.*, 2014, 2015]. For instance, *Rosenqvist and Birkett*, [2002] demonstrated that Synthetic Aperture Radar (SAR) image mosaics can be used to appraise the maximum extents of flooding in the CRB, but were not relevant to assess the SW dynamics and ranges of the variations. *Bwangoy et al.*, [2010] demonstrated the utility of optical and radar remotely sensed data in characterizing the wetlands of the "Cuvette Centrale". They estimated that the wetlands cover an area of 32% in the "Cuvette Centrale", equivalent to 360000 km2.

Crowley et al., [2006], using Gravity Recovery and Climate Experiment (GRACE) data, estimated the terrestrial water storage (surface water storage plus groundwater storage and soil moisture) within the CRB. Over 4 years (2002-2006), the estimate exhibited significant seasonal variations (30±6 mm of equivalent water thickness) and long-term negative trend (~ -70km^3/year). *Lee et al.*, [2011], using GRACE data and other satellite measurements, estimated that the amount of water annually filling and draining the Congo wetlands is about 111 km^3, i.e. one-third the magnitude of the water volumes found on the mainstream Amazon floodplain. *Lee et al.*, [2014], integrating terrestrial water storage (TWS) changes from GRACE, water level changes from radar altimetry, and inundation extents from SAR imagery, quantified TWS change and its surface and subsurface components over the central CRB. They showed that annual variations of the TWS changes during the period of 2007–2010 from 21 to 31 km^3 and are mostly controlled by surface storage changes. *Lee et al.*, [2015] developed water depth maps over the "Cuvette Centrale" based on a linear regression model from altimetry and imagery data. They reported in their study area water storage volumes of about 11 km^3 (Dec-2006), 10 km^3 (Dec-2007), and 9 km^3 (Dec-2008). Finally, *Becker et al.*, [2014] released an unprecedented dataset of water level time series over the entire CRB for the period 2003 to 2009, obtained from the ENVISAT radar altimetry mission. From this unique data set, they proposed an altimeter-based river level height regionalization scheme and thus identified nine distinct hydrological regions in the CRB.

Hence, to supplement this work, we analyze the spatio-temporal variability of SW extent and storage in the CRB, at seasonal and interannual time-scales. For this, along with GIEMS data covering the period 1993-2007, we further develop the observation-based technique combining SWE and radar altimetry measurements [*Frappart et al.*, 2008] to estimate the CRB's SWS variations over the period 2003–2007. The results are evaluated and analyzed along with other *in situ* and remote sensing measurements of three hydrological parameters (discharge, rainfall and terrestrial water storage). The comparisons with the latter will provide, for the first time, the time series of both SW and sub-surface water (SSW) variations distributed throughout the CRB. The paper is structured as follows. In Section 2 we briefly describe the CRB. Section 3 presents the datasets used in this study. In Section 4, we analyze the SWE dynamics from the GIEMS dataset at both seasonal and interannual time-scales for the period 1993 to 2007. Section 5 describes the methodology for deriving SWS from a combination of multi-satellite observations and the results are presented and discussed over the 2003–2007 period. Finally, conclusions and perspectives are presented in Section 6.

2. The study region: The Congo River Basin (CRB)

The CRB is a transboundary basin located in equatorial Africa (Fig. 1). In the heart of the CRB, the shallow depression along the equator is named the "Cuvette Centrale" [*Bernard*, 1945] (Fig. 1). The Congo River begins its course at the Chambeshi River (Fig. 2), rising south of the Lake Tanganyika and transferred by the Bangweulu Swamps. After flowing through Lake Mweru, it joins the Lwalaba River [*Balek*, 1977]. The permanent surface area of Lake Bangweulu is about 3,000 km^2 and can expand to about 15,000 km^2 at the end of the rainy season when its swamps and floodplains get flooded. Lake Mweru covers about 4,650 km^2, and is surrounded by permanent swamps (~1,500 km^2) and floodplains (~900 km^2). The Kasai River from the south, and the Ubangi River from the north are the two principal tributaries of the Congo River. Right-bank tributaries of the Congo River below its junction with the Ubangi include the Likouala aux Herbes, Sangha, Likouala and Alima rivers. Swamp forests predominate on the floodplains in this section [*Beadle*, 1981; *Hughes et al.*, 1992; *Betbeder et al.*, 2014]. The coupled ocean-atmosphere modes of El Niño Southern Oscillation (ENSO) and the Indian Ocean Dipole (IOD) are the main drivers of the CRB hydro-climatic dynamics [*Saji et al.*, 1999; *Behera and Yamagata*, 2001; *Reason*, 2002; *Balas et al.*, 2007; *Hastenrath et al.*, 2007]. In this study, following the drainage patterns and physical characteristics, the CRB has been divided into six sub-basins: Ubangi, Sangha, Middle-Congo, Lower-Congo, Kasai, and Lwalaba. These locations are shown in Fig. 1 and characteristics of the sub-basins are presented in Table 1.

Table 1. Water balance of Congo River Basin, based on [*Bultot*, 1971; *Edwards et al.*, 1983; *Rodier*, 1983; *Olivry et al.*, 1988; *Bricquet*, 1995; *Mahé and Olivry*, 1995; *Laraque et al.*, 2001] (---: Insufficient data to estimate SWS)

Basin name	Drainage area (km^2)	Major rivers and lakes	Mean annual rainfall 1993-2007 (mm)	Mean annual discharge		Mean annual SWE area over 1993-2007 (km^2)		SWS mean annual amplitude (km^3)	Total of SWS flows out the sub-basin (%)
				location	m^3/s	min	max		
Ubangi	651,918	*Uele, Bomu, Ubangi*	1,924	Ubangi mouth	5,936	4,785	7,648	24±4	13±2
Sangha	191,953	*Sangha, Likouala aux herbes*	1,950	Sangha mouth	2,471	1,752	4,668	10±2	13±2
Middle congo	710,758	*Congo, Ruki*	2,164	Above Ubangi	15,484	17,128	24,590	43±7	9±1
Lower congo	144,123	*From Kasai/Congo confluence to the CRB mouth*	1,800	Brazzaville	40,600	464	1,486	---	---
Kasai	884,370	*Kasai, Lukenie, Kwango, Lake Mai-Ndombe*	1,834	Lediba	11,320	10,158	13,003	28±4	8±1
Lwalaba	1,105,879	*Lomani, Lwalaba, Lake Mweru, Lake Tanganyika, Lake Bangweulu*	1,634	Confluence Lomani-Lwalaba	8,358	10,713[a]	37,047[a]	34±4	13±2
TOTAL	**3,689,001**	***CRB***	**1,842**	**Brazzaville**	**40,600**	**47,393**[a]	**78,932**[a]	**81±24**	**6±2**

[a]: The constant surface of the Tanganyika Lake, around 32,600 km^2, is not included.

3. Dataset

3.1. ENVISAT radar altimeter observations

The ENVIronmental SATellite (ENVISAT) was launched in March 2002 by the European Space Agency and its mission was ended in April 2012. The ENVISAT mission carried, among others instruments, a nadir radar altimeter [*Wehr and Attema*, 2001]. Along its ground tracks, repeated every 35 days, we can extract a water level time series, or "virtual stations" (VS), at each intersection with wetlands, large rivers and smaller tributaries of the CRB. The raw ENVISAT data are freely distributed by the Centre for Topographic studies of the Oceans and Hydrosphere [*CTOH*] in along-track Geophysical Data Records (GDRs) format. We used the ice-1 retracker [*Wingham et al.*, 1986; *Bamber*, 1994] as previous showed that it is the more suitable for hydrological studies in terms of accuracy of water levels and availability of the data among the commonly available retracker present in the GDRs [*e.g.,Frappart et al.* 2006; *Santos Da Silva et al.* 2010]. Thus, over 2003-2009, we estimated the water level time series at 350 VS (Fig. 2) using the Virtual ALtimetry Station Tool [*VALS Tool*, 2009] and the Multi-mission Altimetry Processing Software (MAPS). Details about VALS and MAPS procedures can be found in *Santos Da Silva et al.* [2010] and in *Frappart et al.*, [2015a]. All 350 VS passed an efficient and reliable quality control (outlier, gap, shift). As shown in several studies [*Frappart et al.*, 2005; *Santos Da Silva et al.*, 2010; *Papa et al.*, 2012], the accuracy of altimetry derived water levels over inland water bodies is estimated to range between 10 and 40-50 cm on rivers according to the radiometric contrast between the water body and its environment within the radar footprint (vegetation, sand banks, etc …).

3.2. GIEMS surface water extent dynamics

A globally applicable remote-sensing technique has been developed to derive wetland inundation extents: the Global Inundation Extent from Multi-Satellites (GIEMS) [*Prigent* *et al.*, 2001, 2007, 2012, 2016, *Papa et al.*, 2006, 2010]. GIEMS merges: Microwave (19 and 37 GHz) observations from the Special Sensor Microwave/Imager (SSM/I), backscatter at 5.25 GHz from the European Remote Sensing (ERS) scatterometer, and visible (0.58– 0.68 μm) and near-infrared (0.73– 1.1 μm) reflectance from the Advanced Very High Resolution Radiometer (AVHRR) to account for vegetation canopy effects [*Papa et al.*, 2010]. GIEMS, from 1993 to 2007, provides monthly inundation percentage at 0.25° resolution grid cells (each pixel equals 773 km^2). GIEMS dataset has been extensively (i) evaluated at global scale [*Prigent et al.*, 2007; *Papa et al.*, 2008, 2010] and for a broad range of environments [*Frappart et al.*, 2008; *Papa et al.*, 2008, 2013; *Frappart et al.*, 2015b; *Papa et al.*, 2015]; and (ii) used for climatic and hydrological studies, such as the methane surface emissions evaluation [*Bousquet et al.*, 2006; *Ringeval et al.*, 2010] and the river flooding scheme validation coupled with land surface models [*Decharme et al.*, 2008, 2011; *Getirana et al.*, 2012; *Pedinotti et al.*, 2012; *Ringeval et al.*, 2012]. Uncertainties on the inundation estimate from GIEMS is about 10% [*Prigent et al.*, 2007]. In rather densely forested regions, detection of the small areas of surface water can be challenging [*Prigent et al.*, 2007]. This is the case within the CRB, where some regions have very dense vegetation with a network of narrow rivers, such as in the upper part of the Uele River in the Ubangi sub-basin and along the Lukenie and Sankuru Rivers in the Kasai sub-basin. In these regions, when accurate VS are obtained from ENVISAT, but where GIEMS shows limitations in properly delineating the extents of rivers and probably underestimates small wetlands [*Prigent et al.*, 2007], we filled the missing data by distributing 10% of water extent to each river pixel.

Note also that large freshwater bodies such as the Lake Baikal, the Great Lakes, Lake Victoria, and more importantly here for the present study, the Lake Tanganyika, have been masked in the GIEMS database [*Prigent et al.*, 2007]. However, its extent shows small variations on seasonal timescale and does play an important role in the SW dynamics of the

CRB. Nevertheless, its water storage variations will be taken into account when estimating SWS variations (see Section 5).

3.3. Ancillary data

3.3.1. GRACE Regional Solution

The Gravity Recovery And Climate Experiment (GRACE) mission, placed in orbit in March 2002, provides data over the continents and can be used to derive the monthly changes of the terrestrial water storage (TWS) expressed in terms of equivalent water height (EWH) [*Tapley et al.*, 2004]. In this work, we used maps of monthly TWS from the Jet Propulsion Laboratory GRACE land mascon solution (JPL RL05M, available at http://grace.jpl.nasa.gov). This solution proposed some improvements to reduce leakage errors i) across land/ocean boundaries using a Coastline Resolution Improvement filter and ii) for continental hydrology applications providing a set of gain factors. The description of the JPL RL05M solution in detail can be find in *Watkins et al.*, [2015] and *Wiese* [2015]. The dataset resolution is 0.5°x0.5°, but it represents equal-area of 3°x3° spherical caps. In the CRB, the measurement error dominates the leakage error, i.e 5.3 mm vs 2.7 mm respectively of EWH [*Wiese et al.*, 2016]. Over land, the scaled uncertainty derived using methods described in *Wahr et al.*, [1998] are provided and are in the range [0.7 15.8] mm of EWH over the CRB.

3.3.2. Rainfall datasets

CRU TS4.00

We used the Climatic Research Unit (CRU) Time-series (TS) version 4.00 (CRU TS4.00) [*Harris et al.*, 2014; *Harris and Jones*, 2017]. These data are rainfall gridded fields based on monthly observations at meteorological stations across the world's land areas and are provided on high-resolution (0.5x0.5 degree) grids over the period 1901-2015.

GPCP

The Global Precipitation Climatology Project (GPCP, V2.3) monthly dataset is used in this study. This dataset is computed by combining multi-satellite estimates with precipitation gauge information on 2.5° resolution grids from 1979 to present [*Adler et al.*, 2003].

TRMM

The precipitation estimates over the CRB are also obtained from the Tropical Rainfall Measuring Mission (TRMM) 3B43-v7 product [*Huffman et al.*, 2007]. This data set is available since January 1998 at 0.25°×0.25° spatial resolution and at monthly time scale.

3.3.3. In situ gauge stations

We use the daily discharge time series over 1993–2007 at Brazzaville (Fig. 2 15.3°E and 4.3°S, Station: 1070500105 from the Direction de la Gestion des Ressources Hydrauliques (DGRH) - Brazzaville – Congo), Bangui (Fig. 2 18.6°E and 4.36°N Station: 1060700105 from the Direction Générale de L'Hydraulique Service de l'Hydrologie - Bangui - Central African Republic), and Ouesso over 1993-1999 (Fig. 2 16.05°E and 1.61°N Station: 1070800120 from the DGRH).

3.3.4. *Altimeter-derived lake height*

We use the time series of monthly water levels of Lake Mweru (Fig. 2, 28.5°E and 9°S) and Lake Bangweulu (Fig. 2, 29.5°E and 11°S) provided by Hydroweb (http://www.legos.obs-mip.fr/fr/soa/hydrologie/hydroweb/). Hydroweb is developed by the Laboratoire d'Etudes en Géophysique Océanographie Spatiales (LEGOS) in France and provides water level time series of selected water bodies (rivers, lakes, reservoirs and wetlands) worldwide using the merged data from the Topex/Poseidon, Jason-1, Jason-2, Jason-3, ERS2, ENVISAT, SARAL and Geosat Follow-On (GFO) satellite missions. The processing procedure details of Hydroweb can be found in *Crétaux et al.*, [2011].

4. Spatio-temporal variations of surface water extent (SWE)

The mean and maximum of the SWE per grid cell over 1993 to 2007 are displayed in Figs. 3a and 3b. A very realistic spatial distribution of the major rivers (Congo, Kasai, Ubangi and Lwalaba) and some tributaries is shown by these maps. Associated inundated areas, wetlands and the region of the "Cuvette Centrale" are also well delineated. Maxima are located in two regions: (i) in the Lwalaba basin, mainly along the major lakes; and (ii) in the "Cuvette Centrale" along the Congo main stream, between 15°-18°E and 0°-2.5°S, including Lake Mai-Ndombe and Lake Tumba. The SWE and precipitation seasonal variations are presented in Fig. 4 and in Table 1. In this analysis, we computed the monthly rainfall averages over 1993-2007 from CRU TS4.00, GPCP and TRMM products. In Ubangi, Sangha and Middle Congo sub-basins, the precipitation dynamics present a bimodal distribution, which is not observed in the SWE seasonal variations. However, SWE in Ubangi and Middle Congo follow slowly the overall increase trend of precipitation from April to November. The SWE in Sangha presents a sharp increase from September to November. The SWE in these three sub-basins drops a month after the beginning of the precipitation decrease and reaches their minima 2-3 months after those of precipitation. These three sub-basins see their flooded area increase two to three-fold on average over the year. For instance, in the Middle Congo, the flooded areas vary from 16,700 km^2 at low waters to 26,000 km^2 at high waters. The SWE in Kasai shows very little variations over the year, probably due to the low GIEMS data coverage in this specific area. In the Lower Congo, between August and December, the SWE drops a month after the beginning of the precipitation decrease and reach its minimum 3 months after the precipitation minimum.

The flood period generally occurs between October and November and is perfectly in phase with the precipitation dynamics.

The SWE dynamics over 1993-2007 is also compared to: (i) the *in situ* river discharge measured at Brazzaville, Bangui and Ouesso (Fig. 5, see Fig. 2 for their locations) and (ii) satellite altimeter-derived height at Mweru, Bangweulu and Mai-Ndombe lakes (Fig. 6, see Fig. 2 for their locations). In Fig. 5, the river discharge time series of Brazzaville is compared to the total area of SWE in the "Cuvette Centrale", i.e. [15-20°E 3-0°S] and the Bangui and Ouesso discharge time series are compared to the total area of SWE in the Ubangui and Sangha sub-basins respectively. Fig. 5 a, b, and c show that the annual variability of each river discharge time series are closely connected to the SWE dynamics, with high correlation coefficients ($r \geq 0.8$). At Bangui and Ouesso, the discharge peak occurs one month before the SWE maximum.

In the following, we removed seasonal variation from the time series by using a 12-month moving average. The interannual deseasonalized anomalies of the discharge and SWE time series are presented in Fig. 5 d, e, and f. We obtain a moderate agreement ($r>0.5$) in the interannual temporal patterns between the two variables in the three locations. These SWE interannual patterns probably result in a nonlinear relationship between the discharges and other parameters of the water balance, such as groundwater levels. In addition surface water residence time could also be influenced by the size and depth of the drainage systems, and by the connection/disconnection regimes between main streams and associated inundation zones. Further investigations are needed to clarify these dynamics.

The time series of 3 lakes height variations (Mai-Ndombe, Mweru, Bangweulu) are compared in Fig. 6 with the cumulated SWE dynamics around the area. It shows that lake height variations and the SWE are generally well correlated ($r \geq 0.8$, Fig. 6 a,b,c) at seasonal timescales with a delay lag of 1 and 2 months for the Bangweulu and the Mweru, respectively. At an interannual timescale, Fig 6 (d,e,f) also show high correlation ($r \geq 0.7$) between the anomalies of the two variables, especially over the Mweru Lake. Over Mweru, three particular events are noticeable in 1997-1998, 2000-2001 and 2006-2007 (November to May period). Because of shorter time series, only the 2006-2007 event is noticeable for the Mai-Ndombe and Bangweulu lakes. The periods 1997-1998 and 2006-2007 are characterized by positive Indian Ocean Dipole (pIOD) events in conjunction with an El Niño event [*Ummenhofer et al.*, 2009]. In general, pIOD events induce large rainfall deficit in the eastern Indian Ocean and Indonesia, and floods in western Indian Ocean, South India, and East Africa [*McPhaden*, 2002]. During those events, the Mweru SWE reaches record high extent (2,700 km^2 and 1,900 km^2) associated with large positive anomalies in the water level of the lake (Fig. 6 d and e).

In order to better characterize SWE interannual variability and its possible relation with large climate events, we further analyze the deseasonalized anomalies between 1993 and 2007 (Fig. 7). The SWE interannual variability over the Ubangi, Kasai, Middle Congo and Lower Congo show the same dynamics (Fig 7a). A large negative anomaly in SWE is observed from 1998 to 2000, which could be associated with the 1998-2000 persistent La Niña event. This type of event is often linked to drier than normal conditions over equatorial East Africa [*McPhaden*, 2002]. The SWE interannual variability over the Lwalaba basin (Fig. 7c) presents a large positive event in 1997/1998, previously observed in the Mweru Lake height variations (Fig. 6b/e), where a pIOD event (associated with an excess of rain in western Indian Ocean, South India, and East Africa) occurs in conjunction with an El Niño event [*Ummenhofer et al.*, 2009]. For example, after the 1997 pIOD event, the level of Lake Victoria rose by 1.7 m, Lake Tanganyika by 2.1 m and Lake Malawi by

1.8 m; the Sudd marshes levels also rose [*Birkett et al.*, 1999; *Becker et al.*, 2010] and very high river flows were measured at Kinshasa [*Conway et al.*, 2005]. Moreover, these devastating floods have resulted in several thousand deaths and hundreds of thousands people have been displaced in Kenya, Somalia, Sudan, Uganda, and Ethiopia [*Cai et al.*, 2014]. In the Lwalaba basin, the SWE increased significantly by a factor of ~4 from late 1997 to the end of 1998.

5. Spatio-temporal variations of surface water storage (SWS)

Here we present the spatio-temporal variability of SWS estimated by combining the SWE from GIEMS with the 350 altimeter-derived water level heights. The two-step methodology is described briefly in the following sections and we refer to *Frappart et al.*, [2008, 2011] for more details. The results are analyzed for 2003-2007, the common period of availability for both datasets.

5.1. Monthly maps of surface water level anomalies

Monthly maps of water level in the CRB were obtained by combining GIEMS and ENVISAT derived water levels. Following *Frappart et al.* [2008, 2011], water levels for a given month were linearly interpolated over GIEMS inundation. Each SW level map had a spatial resolution of 0.25°×0.25°, and the elevation of each pixel is given with reference to a map of minimum SW levels estimated over 2003–2007 using a hypsometric approach (see Fig. S1 from *Frappart et al.*, [2012]). For each inundated pixel of coordinates (λ_j, φ_j), the minimum elevation is given as :

$$h_{min}\left(\lambda_j, \varphi_j, \alpha, \Delta T\right) = min\left(h\left(\lambda_j, \varphi_j, t\right)\right)_{P\left(\lambda_j, \varphi_j, t\right) \le \alpha; t \epsilon \Delta T} \quad (1)$$

where h_{min} is the minimum elevation (m) during the observation period ΔT for a percentage of inundation α from GIEMS, which varies between 0 and 100 and t is a monthly observation during ΔT.

Fig. 8 shows the seasonal evolution of surface water heights (SWH) in the CRB sub-basins for the period August 2006 to May 2007 covering a pIOD-El Niño event. In the Ubangi and Sangha basins the SWH increase in August-October (up to 4 m) and reach their maximum values in November (up to 6 meters). In the Middle Congo River Basin, SWH increase from October to December and show an important spatial variability. The SWH highest values (~3 m) are along the Congo River mainstream and in the south of the basin along the Ruki River. From January, we observe increases in the southern part of the CRB basin. In the upper Lwalaba basin we observe from January to March an important inundation zone (up to 4 m). From April, the SWH start to decline. The monthly maps of SWH are now used to estimate surface water storage expressed as volumes for 2003–2007.

5.2. Monthly time series of surface water volume variations

Following *Frappart et al.* [2008, 2011], the time variations of SW volume, are computed as :

$$V_{SW}(t) = R_e^2 \sum_{j\epsilon S} P\left(\lambda_j, \varphi_j, t\right)\left(h\left(\lambda_j, \varphi_j, t\right) - h_{min}\left(\lambda_j, \varphi_j\right)\right)\cos\left(\varphi_j\right)\Delta\lambda\Delta\varphi \qquad (2)$$

where V_{SW} is the volume (km^3) of SW, R_e the earth's radius (6378 km), $P\left(\lambda_j, \varphi_j, t\right)$, $h\left(\lambda_j, \varphi_j, t\right)$, $h_{min}\left(\lambda_j, \varphi_j\right)$ are respectively the percentage of inundation, the water level at time t, and the minimum of water level at the pixel $\left(\lambda_j, \varphi_j\right)$; $\Delta\lambda$ and $\Delta\varphi$ are respectively the grid steps in longitude and latitude. Monthly surface water storage (SWS) fluctuations are estimated for over 2003–2007.

For lakes Bangweulu, Mai-Ndombe and Mweru, surface water volume anomalies ΔV_{SW} were computed following Baup et al. [2014]:

$$\Delta V_{SW}(t) = S(t-1)|\Delta h(t)| + sgn(\Delta h(t))\frac{|\Delta S(t)||\Delta h(t)|}{2} \qquad (3)$$

Where *ΔS(t)=S(t)-S(t-1)* and *Δh(t)=h(t)-h(t-1)* are the variations of the surface and height of the lake between instants *t* and *t-1* respectively.

For Lake Tanganiyka, anomalies of water volume were simply estimated multiplying the surface of the lake (32,600 km² from *Spigel and Coulter*, 1996) by the anomaly of water stage obtained using ENVISAT altimetry data.

The volume of SW is the sum of the contributions of the water volume contained in the floodplains and the lakes of the CRB. Accordingly, the time variations of *TWS* ($V_{TWS}(t)$) anomalies are computed following *Ramillien et al.*, [2005]:

$$\Delta V_{TWS}(t) = R_e^2 \sum_{j\in S} \Delta h_{TWS}\left(\lambda_j, \varphi_j, t\right) \cos\left(\varphi_j\right) \Delta\lambda\Delta\varphi \qquad (4)$$

where $h_{TWS}(\lambda_j,\varphi_j,t)$ is the equivalent height anomaly of *TWS* (km^3) at time *t* of the pixel of coordinates (λ_j,φ_j), R_e the earth's radius (6378 km), $\Delta\lambda$ and $\Delta\varphi$ are respectively the grid steps in longitude and latitude. The maximum error for the SW volume variation (km^3), ΔV, is estimated as :

$$\max(\Delta V) = S_{max}\Delta\delta h_{max} + \Delta S_{max}\delta h_{max} \qquad (5)$$

where S_{max} is the maximum flooded surface (km^2), δh_{max} is the maximum SWH variation (km) between two consecutive months, ΔS_{max} is the maximum error for the flooded surface (km^2) and $\Delta\delta h_{max}$ is the maximum dispersion (km) of the SWH between two consecutive months.

Fig. 9 presents the spatial patterns of SWS changes, estimated as the year among the five years being the maximum range of SWS. It shows realistic spatial structures along the Congo River and the "Cuvette Centrale", as well as in the Tumba and Mai-Ndombe lakes, where annual maximum storage variations reach up to 1.3 km^3/year per grid cell.

Secondary maxima are observed in the Lwalaba basin around the lakes Kivu and Bangweulu and along the Lwalaba River upstream, with SWS varying between 0.3–0.6 km^3/year per grid cell. Low SWS changes are observed in other locations of CRB (below 0.2 km^3/year), in accordance with very low variations in water levels observed in the altimetry measurements.

To illustrate the interannual variability at the basin-scale, Fig. 10 shows the yearly variations of SWS, as a percentage of the difference from median computed 2003-2007. It reveals rather strong year-to-year and spatial variability. For instance, during the 2007 pIOD/El Niño year, a clear positive anomaly of SWS is observed all over the CRB basin. During 2003, a pIOD year, increases in SWS are observed along the Ubangi river mainstream and along the north part of the Lwalaba River whereas a deficit of SWS is observed in the Kasai sub-basin. Conversely, in 2004, one notices positive anomalies of SWS of about 80-100% in the Kasai sub-basin whereas a negative anomaly is observed in the rest of CRB.

For the entire CRB over 2003-2007, on average the annual SWS amplitude is 81±24 km^3 (Fig. 11 and Table 1). A significant year-to-year variation is observed, with for instance an annual amplitude of ~57 km^3 in 2003 whereas the amplitude reaches 114 km^3 in 2006. That corresponds to 6±2 % of the total fresh water volume that flows out annually from the CRB as river discharge into the Atlantic Ocean with a mean flow of ~ 40,600 m^3/s (i.e. ~1,280 km^3/year). As a comparison, the Amazon River SWS annual variation corresponds to ~15% of the total fresh water volume that flows out annually of its basin as river discharge [*Frappart et al.*, 2012]. In the Ubangi basin, the mean annual SWS amplitude 24±4 km^3, with a minimum of ~20 km^3 observed in 2004 and a maximum of ~30 km^3 in 2007. We report an annual mean SWS amplitude of 10±2 km^3 for the Sangha and 28±4

km^3 for the Kasai. The Middle Congo presents a mean annual SWS amplitude of 43±7 km^3, with a minimum of ~34 km^3 observed in 2003 and a maximum of ~52 km^3 in 2007. In contrast, the Lwalaba basin shows an annual SWS minimum of ~30 km^3 observed in 2007 and a maximum of ~41 km^3 in 2005. On average this basin shows a mean annual SWS amplitude of 34±4 km^3, where we have included the volume variations of Bangweulu, Mweru and Tanganyika Lakes obtained from the combination of altimetry and GIEMS. We estimated the maximum error for the SWS change in the CRB using Equation (5) and using the following values: S_{max} = 78 932 km^2 in February, 2007; δh_{max} = 0.6 m, mean maximum SWH change between two consecutive months during 2003-2007; ΔS_{max} = 10% from *Prigent et al.*, [2007] of 78 932 km^2; and $\Delta\delta h_{max}$ = 0.2 m, maximum average dispersion of the SWH in 2007. We obtain a maximum error of ~20 km^3 for an annual variation of 76 km^3 in 2007, i.e., an error of ~26%. This value is of the same order of magnitude as that obtained over the Rio Negro (~23% *Frappart et al.*, [2008]), over the Orinoco Basin (~30%, *Frappart et al.*, [2015b]) and over the Ganges-Brahmaputra Basin (~24%, *Papa et al.*, [2015]). In the same way, we obtained over the sub-basins the maximum errors of ~17% for the Ubangui, ~23% for the Sangha, ~17% for the Middle Congo, ~19% over the Kasai, and ~27% over the Lwalaba. Respectively, the mean annual variation in SWS represents 13±2 % of the total volume of water that flows out the Ubangi basin and at the Sangha mouth, 8±1 % at the Kasai mouth, 9±1 % along the Congo River above the Ubangi mouth and ~13±2% at the Lwalaba mouth.

In Fig 11, we compared the SWS and TWS from the GRACE solution. For the entire CRB, the correlation between the SWS and TWS is ~0.8 and the SWS preceded TWS by one month. The seasonal SWS variations, estimated as the ratio between the mean amplitude of SWS and TWS variations over the study period, represent 10±1 % of the TWS variations in the Ubangi basin, 18±1% in the Sangha, 33±7 % in the Middle Congo, encompassing extensive floodplains and Lake Tumba, and 12±2 % in the Lwalaba sub-basins. For the entire CRB, the seasonal SWS variations represent 19±5 % of the TWS variations. As a comparison, using the same approach, the seasonal contribution of SWS to TWS variations were found to be of ~43% for the Amazon [*Frappart et al.*, 2012] and 45% in the Ganges-Brahmaputra basin [*Papa et al.*, 2015].

We subtract SWS to TWS in order to obtain the ''sub-surface water storage'' variations (Sub-SWS, Fig.11) defined as the sum of soil moisture and groundwater. We assume that the variations in water storage compartments derived from canopy are negligible over the 2003-2007 in the CRB and hence are not considered here. The Sub-SWS contribution (Fig.11) in the Ubangi, Sangha and Lwalaba basins is very important and suggests that the hydrological compartments, such as soil moisture and groundwater, have a major influence on TWS. On the contrary, in the Middle Congo, the SWS alone contributes over one-third of the TWS variations over this sub-basin.

6. Conclusions and perspectives

This work presents an unparalleled analysis of the dynamics of surface water extent (1993–2007) and storage (2003-2007) in the CRB. First, we show that the SWE seasonal patterns from GIEMS dataset exhibit very realistic distributions of major rivers (Congo, Kasai, Ubangi and Lwalaba) and their tributaries, with two maxima located: i) in the lake region of the Lwalaba sub-basin and ii) in the "Cuvette Centrale", including Tumba and Mai-Ndombe Lakes. For the period 1993-2007, we found a ENSO/IOD influence on the SWE interannual variability. Following the approach developed by *Frappart et al.* [2008, 2011], we combined GIEMS observations with inland water level variations from ENVISAT radar altimetry (350 observations on the rivers) to analyze the variations of fresh water stored in the CRB different hydrological compartments. Overall, during 2003-2007, the annual mean variation in SWS was 81±24 km^3 and contributes to 19±5 % of the annual variations of GRACE-derived TWS. It represents also 6±2 % of the annual fresh water volume that flows from the CRB into the Atlantic Ocean. Finally, we can mention the very different behavior in the Middle Congo River Basin, where SWS alone contributes more than one-third of the TWS variations over this sub-basin. It is important to note that the spatial-resolution sampling of the altimetry-based virtual station dataset could be increased using ENVISAT and ERS archives, especially with the recent reprocessing devoted land water studies made available by CTOH [*Frappart et al.*, 2016] and temporal extended using current altimetry satellites including Jason-1 (GDR E), Jason-2, Jason-3, SARAL, and Sentinel-3A, as well as future missions such as Sentinel-3B (to be launched in 2017), Sentinel-6/Jason-CS (Jason-CS A and B planned for 2020 and 2026, respectively). This new surface water storage (and sub-surface water storage) dataset for the CRB over 5 years is a further step towards improving our knowledge of climatic and hydrological processes in this region. This new surface water storage (and sub-surface water storage) dataset for the CRB over 5 years is a further step towards improving our knowledge of climatic and hydrological processes in this region. It is an unprecedented source of information for hydrological modeling of the CRB as well as a baseline in the definition and validation of future hydrology-oriented satellite missions such as the NASA-CNES Surface Water Ocean Topography (SWOT) to be launched in 2021, which will be dedicated to global surface hydrology. More generally, these results on the large scale CRB's hydro-climate processes, in addition to improving our fundamental knowledge about this major hydrologic basin, offer an unique opportunity for conducting many new studies in Africa by using even larger datasets, with a focus on a clear gain for the management of water resources in this continent.

Acknowledgments

This study was funded by CNES TOSCA project “Monitoring of terrestrial water storage variability in the Tropics. An integrated approach of multi-satellite observations, in situ measurements and modeling (HyVarMultiObs)” (2012-2015).

References

Achard, F., H. D. Eva, H.-J. Stibig, P. Mayaux, J. Gallego, T. Richards, and J.-P. Malingreau (2002), Determination of deforestation rates of the world’s humid tropical forests, *Science*, *297*(5583), 999–1002.

Adler, R. F. et al. (2003), The version-2 global precipitation climatology project (GPCP) monthly precipitation analysis (1979–present), *Journal of hydrometeorology*, *4*(6), 1147–1167.

Alsdorf, D., E. Beighley, A. Laraque, H. Lee, R. Tshimanga, F. O’Loughlin, G. Mahe, D. Bienvenu, G. Moukandi, and R. G. M. Spencer (2016), Opportunities for Hydrologic Research in the Congo Basin, *Rev. Geophys.*, 2016RG000517, doi:10.1002/2016RG000517.

Alsdorf, D. E., E. Rodríguez, and D. P. Lettenmaier (2007), Measuring surface water from space, *Reviews of Geophysics*, *45*(2), doi:10.1029/2006RG000197.

Balas, N., S. E. Nicholson, and D. Klotter (2007), The relationship of rainfall variability in West Central Africa to sea-surface temperature fluctuations, *International journal of climatology*, *27*(10), 1335–1349.

Balek, J. (1977), *Hydrology and water resources in tropical Africa*, Elsevier.

Bamber, J. L. (1994), Ice sheet altimeter processing scheme, *International Journal of Remote Sensing*, *15*(4), 925–938, doi:10.1080/01431169408954125.

Baup, F., F. Frappart, and J. Maubant (2014), Combining high-resolution satellite images and altimetry to estimate the volume of small lakes, *Hydrol. Earth Syst. Sci.*, *18*(5), 2007–2020, doi:10.5194/hess-18-2007-2014.

Beadle, L. C. (1981), *The inland waters of Africa. An introduction to tropical limnology*, Longman, London.

Becker, M., W. LLovel, A. Cazenave, A. Güntner, and J.-F. Crétaux (2010), Recent hydrological behavior of the East African great lakes region inferred from GRACE, satellite altimetry and rainfall observations, *Comptes Rendus Geoscience*, *342*(3), 223–233.

Becker, M., J. da Silva, S. Calmant, V. Robinet, L. Linguet, and F. Seyler (2014), Water Level Fluctuations in the Congo Basin Derived from ENVISAT Satellite Altimetry, *Remote Sensing*, *6*(10), 9340–9358, doi:10.3390/rs6109340.

Behera, S. K., and T. Yamagata (2001), Subtropical SST dipole events in the southern Indian Ocean, *Geophys. Res. Lett.*, *28*(2), 327–330, doi:10.1029/2000GL011451.

Beighley, R. E., R. L. Ray, Y. He, H. Lee, L. Schaller, K. M. Andreadis, M. Durand, D. E. Alsdorf, and C. K. Shum (2011), Comparing satellite derived precipitation datasets using the Hillslope River Routing (HRR) model in the Congo River Basin, *Hydrological Processes*, *25*(20), 3216–3229.

Bele, Y., E. Mulotwa, B. Bokoto de Semboli, D. Sonwa, and A. M. Tiani (2010), Central Africa: the effects of climate change in the Congo Basin; the need to support local adaptive capacity,

Bernard, É. (1945), *Le climat écologique: de la cuvette centrale congolaise*.

Betbeder, J., V. Gond, F. Frappart, N. N. Baghdadi, G. Briant, and E. Bartholome (2014), Mapping of Central Africa Forested Wetlands Using Remote Sensing, *IEEE Journal of Selected Topics in Applied Earth Observations and Remote Sensing*, *7*(2), 531–542, doi:10.1109/JSTARS.2013.2269733.

Birkett, C., R. Murtugudde, and T. Allan (1999), Indian Ocean climate event brings floods to East Africa’s lakes and the Sudd Marsh, *Geophysical Research Letters*, *26*(8), 1031–1034.

Birkett, C. M. (1995), The contribution of TOPEX/POSEIDON to the global monitoring of climatically sensitive lakes, *Journal of Geophysical Research: Oceans*, *100*(C12), 25179–25204.

Bousquet, P. et al. (2006), Contribution of anthropogenic and natural sources to atmospheric methane variability, *Nature*, *443*(7110), 439–443, doi:10.1038/nature05132.

Bricquet, J.-P. (1995), Les écoulements du Congo à Brazzaville et la spatialisation des apports, in *Grands* *bassins fluviaux périatlantiques : Congo, Niger, Amazone*, edited by J. Boulègue, J.-C. Olivry, and Grands Bassins Fluviaux Péri-Atlantiques : Congo, Niger, Amazone, Paris (FRA), 1993/11/22-24, pp. 27–38, ORSTOM, Paris.

Brown, H. C. P., B. Smit, O. A. Somorin, D. J. Sonwa, and J. N. Nkem (2014), Climate change and forest communities: prospects for building institutional adaptive capacity in the Congo Basin forests, *Ambio*, *43*(6), 759–769.

Bultot, F. (1971), *Atlas climatique du bassin congolais*, INEAC.

Bwangoy, J.-R. B., M. C. Hansen, D. P. Roy, G. D. Grandi, and C. O. Justice (2010), Wetland mapping in the Congo Basin using optical and radar remotely sensed data and derived topographical indices, *Remote Sensing of Environment*, *114*(1), 73–86, doi:10.1016/j.rse.2009.08.004.

Cai, W., A. Santoso, G. Wang, E. Weller, L. Wu, K. Ashok, Y. Masumoto, and T. Yamagata (2014), Increased frequency of extreme Indian Ocean Dipole events due to greenhouse warming, *Nature*, *510*(7504), 254–258, doi:10.1038/nature13327.

Calmant, S., F. Seyler, and J. F. Cretaux (2008), Monitoring continental surface waters by satellite altimetry, *Surveys in geophysics*, *29*(4–5), 247–269.

Camberlin, P., S. Janicot, and I. Poccard (2001), Seasonality and atmospheric dynamics of the teleconnection between African rainfall and tropical sea-surface temperature: Atlantic vs. ENSO, *International Journal of Climatology*, *21*(8), 973–1005.

Conway, D., E. Allison, R. Felstead, and M. Goulden (2005), Rainfall variability in East Africa: implications for natural resources management and livelihoods, *Philosophical Transactions of the Royal Society of London A: Mathematical, Physical and Engineering Sciences*, *363*(1826), 49–54.

Crétaux, J.-F., and C. Birkett (2006), Lake studies from satellite radar altimetry, *Comptes Rendus Geoscience*, *338*(14), 1098–1112.

Crétaux, J.-F., S. Calmant, R. A. Del Rio, A. Kouraev, M. Bergé-Nguyen, and P. Maisongrande (2011), Lakes studies from satellite altimetry, in *Coastal Altimetry*, pp. 509–533, Springer.

Crétaux, J.-F., R. Abarca-del-Río, M. Berge-Nguyen, A. Arsen, V. Drolon, G. Clos, and P. Maisongrande (2016), Lake Volume Monitoring from Space, *Surveys in Geophysics*, *37*(2), 269–305.

Crowley, J. W., J. X. Mitrovica, R. C. Bailey, M. E. Tamisiea, and J. L. Davis (2006), Land water storage within the Congo Basin inferred from GRACE satellite gravity data, *Geophysical Research Letters*, *33*(19), L19402.

CTOH (n.d.), Center for Topographic studies of the Ocean and Hydrosphere., Available from: http://ctoh.legos.obs-mip.fr/ (Accessed 26 April 2016)

Dargie, G. C., S. L. Lewis, I. T. Lawson, E. T. Mitchard, S. E. Page, Y. E. Bocko, and S. A. Ifo (2017), Age, extent and carbon storage of the central Congo Basin peatland complex, *Nature*.

Decharme, B., H. Douville, C. Prigent, F. Papa, and F. Aires (2008), A new river flooding scheme for global climate applications: Off-line evaluation over South America, *J. Geophys. Res.*, *113*(D11), D11110, doi:10.1029/2007JD009376.

Decharme, B., R. Alkama, F. Papa, S. Faroux, H. Douville, and C. Prigent (2011), Global off-line evaluation of the ISBA-TRIP flood model, *Clim Dyn*, *38*(7–8), 1389–1412, doi:10.1007/s00382-011-1054-9.

Edwards, K. A., G. A. Classen, E. H. J. Schroten, and others (1983), The water resource in tropical Africa and its exploitation,

Frappart, F., F. Seyler, J.-M. Martinez, J. G. León, and A. Cazenave (2005), Floodplain water storage in the Negro River basin estimated from microwave remote sensing of inundation area and water levels, *Remote Sensing of Environment*, *99*(4), 387–399, doi:10.1016/j.rse.2005.08.016.

Frappart, F., S. Calmant, M. Cauhopé, F. Seyler, and A. Cazenave (2006), Preliminary results of ENVISAT RA-2-derived water levels validation over the Amazon basin, *Remote Sensing of Environment*, *100*(2), 252–264, doi:10.1016/j.rse.2005.10.027.

Frappart, F., F. Papa, J. S. Famiglietti, C. Prigent, W. B. Rossow, and F. Seyler (2008), Interannual variations of river water storage from a multiple satellite approach: A case study for the Rio Negro River basin, *Journal of Geophysical Research: Atmospheres*, *113*(D21).

Frappart, F., F. Papa, A. Güntner, W. Susanna, G. Ramillien, C. Prigent, W. B. Rossow, and M.-P. Bonnet

(2010), Interannual variations of the terrestrial water storage in the Lower Ob'Basin from a multisatellite approach, *Hydrology and Earth System Sciences Discussions*, *14*(12), 2443–2453.

Frappart, F. et al. (2011), Satellite-based estimates of groundwater storage variations in large drainage basins with extensive floodplains, *Remote Sensing of Environment*, *115*(6), 1588–1594, doi:10.1016/j.rse.2011.02.003.

Frappart, F., F. Papa, J. S. da Silva, G. Ramillien, C. Prigent, F. Seyler, and S. Calmant (2012), Surface freshwater storage and dynamics in the Amazon basin during the 2005 exceptional drought, *Environ. Res. Lett.*, *7*(4), 044010, doi:10.1088/1748-9326/7/4/044010.

Frappart, F., F. Papa, V. Marieu, Y. Malbeteau, F. Jordy, S. Calmant, F. Durand, and S. Bala (2015a), Preliminary Assessment of SARAL/AltiKa Observations over the Ganges-Brahmaputra and Irrawaddy Rivers, *Marine Geodesy*, *38*(sup1), 568–580, doi:10.1080/01490419.2014.990591.

Frappart, F., F. Papa, Y. Malbeteau, J. G. León, G. Ramillien, C. Prigent, L. Seoane, F. Seyler, and S. Calmant (2015b), Surface Freshwater Storage Variations in the Orinoco Floodplains Using Multi-Satellite Observations, *Remote Sensing*, *7*(1), 89–110.

Frappart, F., B. Legrésy, F. Nino, F. Blarel, N. Fuller, S. Fleury, F. Birol, and S. Calmant (2016), An ERS-2 altimetry reprocessing compatible with ENVISAT for long-term land and ice sheets studies, *Remote Sensing of Environment*, *184*, 558–581.

Getirana, A. C. V., A. Boone, D. Yamazaki, B. Decharme, F. Papa, and N. Mognard (2012), The Hydrological Modeling and Analysis Platform (HyMAP): Evaluation in the Amazon Basin, *J. Hydrometeor*, *13*(6), 1641–1665, doi:10.1175/JHM-D-12-021.1.

Harris, I., P. D. Jones, T. J. Osborn, and D. H. Lister (2014), Updated high-resolution grids of monthly climatic observations - the CRU TS3.10 Dataset: UPDATED HIGH-RESOLUTION GRIDS OF MONTHLY CLIMATIC OBSERVATIONS, *International Journal of Climatology*, *34*(3), 623–642, doi:10.1002/joc.3711.

Harris, I. C., and P. D. Jones (2017), CRU TS4.00: Climatic Research Unit (CRU) Time-Series (TS) version 4.00 of high resolution gridded data of month-by-month variation in climate (Jan. 1901- Dec. 2015). Centre for Environmental Data Analysis., *University of East Anglia Climatic Research Unit*, doi:10.5072/edf8febfdaad48abb2cbaf7d7e846a86.

Hastenrath, S. (1985), *Climate and circulation of the tropics*, Springer Netherlands, Dordrecht.

Hastenrath, S., D. Polzin, and C. Mutai (2007), Diagnosing the 2005 drought in equatorial East Africa., *Journal of Climate*, *20*(18).

Huffman, G. J., R. F. Adler, D. T. Bolvin, G. Gu, E. J. Nelkin, K. P. Bowman, Y. Hong, E. F. Stocker, and D. B. Wolff (2007), The TRMM Multisatellite Precipitation Analysis (TMPA): Quasi-global, multiyear, combined-sensor precipitation estimates at fine scales., *Journal of Hydrometeorology*, *8*(1).

Hughes, R. H., J. S. Hughes, and G. M. Bernacsek (1992), *A directory of African wetlands*, IUCN.

Jung, H. C., J. Hamski, M. Durand, D. Alsdorf, F. Hossain, H. Lee, A. K. M. Hossain, K. Hasan, A. S. Khan, and A. K. M. Hoque (2010), Characterization of complex fluvial systems using remote sensing of spatial and temporal water level variations in the Amazon, Congo, and Brahmaputra Rivers, *Earth Surface Processes and Landforms*, *35*(3), 294–304.

Laraque, A., G. Mahé, D. Orange, and B. Marieu (2001), Spatiotemporal variations in hydrological regimes within Central Africa during the XXth century, *Journal of Hydrology*, *245*(1), 104–117.

Laraque, A., J. P. Bricquet, A. Pandi, and J. C. Olivry (2009), A review of material transport by the Congo River and its tributaries, *Hydrological processes*, *23*(22), 3216–3224.

Lee, H., R. E. Beighley, D. Alsdorf, H. C. Jung, C. K. Shum, J. Duan, J. Guo, D. Yamazaki, and K. Andreadis (2011), Characterization of terrestrial water dynamics in the Congo Basin using GRACE and satellite radar altimetry, *Remote Sensing of Environment*, *115*(12), 3530–3538.

Lee, H., H. C. Jung, T. Yuan, R. E. Beighley, and J. Duan (2014), Controls of terrestrial water storage changes over the central Congo Basin determined by integrating PALSAR ScanSAR, Envisat altimetry, and GRACE data, *Remote Sensing of the Terrestrial Water Cycle*, *206*, 117.

Lee, H., T. Yuan, H. C. Jung, and E. Beighley (2015), Mapping wetland water depths over the central Congo Basin using PALSAR ScanSAR, Envisat altimetry, and MODIS VCF data, *Remote Sensing of Environment*, *159*, 70–79.

Mahé, G., and J.-C. Olivry (1995), Variations des précipitations et des écoulements en Afrique de l'Ouest et centrale de 1951 à 1989, *Science et changements planétaires/Sécheresse*, *6*(1), 109–117.

Mahé, G., and J.-C. Olivry (1999), assessment of freshwater yields to the ocean along the intertropical Atlantic coast of Africa (1951–1989), *Comptes Rendus de l'Académie des Sciences-Series IIA-Earth and Planetary Science*, *328*(9), 621–626.

McPhaden, M. J. (2002), El Ni no and La Ni na: Causes and Global Consequences, *Encyclopedia of global environmental change*, *1*, 1–17.

Olivier, J., G. Janssens-Maenhout, M. Muntean, and J. Peters (2016), *Trends in global CO2 emissions; 2016 Report*, The Hague: PBL Netherlands Environmental Assessment Agency; Brussels: Joint Research Centre.

Olivry, J.-C., J.-P. Bricquet, J.-P. Thiébaux, L. Sigha-Nkamdjou, and Sediment Budgets : Symposium, Porto-Alegre (BRA), 1988/12 (1988), Transport de matière sur les grands fleuves des régions intertropicales : les premiers résultats des mesures de flux particulaires sur le bassin du fleuve Congo, in *Sediment budgets*, vol. 174, pp. 509–521, AISH, Wallingford.

O'Loughlin, F., M. A. Trigg, G.-P. Schumann, and P. D. Bates (2013), Hydraulic characterization of the middle reach of the Congo River, *Water Resources Research*, *49*(8), 5059–5070.

Papa, F., C. Prigent, F. Durand, and W. B. Rossow (2006), Wetland dynamics using a suite of satellite observations: A case study of application and evaluation for the Indian Subcontinent, *Geophys. Res. Lett.*, *33*(8), L08401, doi:10.1029/2006GL025767.

Papa, F., A. Güntner, F. Frappart, C. Prigent, and W. B. Rossow (2008), Variations of surface water extent and water storage in large river basins: A comparison of different global data sources, *Geophysical Research Letters*, *35*(11).

Papa, F., C. Prigent, F. Aires, C. Jimenez, W. B. Rossow, and E. Matthews (2010), Interannual variability of surface water extent at the global scale, 1993–2004, *Journal of Geophysical Research: Atmospheres*, *115*(D12).

Papa, F., S. K. Bala, R. K. Pandey, F. Durand, V. V. Gopalakrishna, A. Rahman, and W. B. Rossow (2012), Ganga-Brahmaputra river discharge from Jason-2 radar altimetry: An update to the long-term satellite-derived estimates of continental freshwater forcing flux into the Bay of Bengal, *J. Geophys. Res.*, *117*(C11), C11021, doi:10.1029/2012JC008158.

Papa, F., F. Frappart, A. Güntner, C. Prigent, F. Aires, A. C. Getirana, and R. Maurer (2013), Surface freshwater storage and variability in the Amazon basin from multi-satellite observations, 1993–2007, *Journal of Geophysical Research: Atmospheres*, *118*(21), 11–951.

Papa, F. et al. (2015), Satellite-derived surface and sub-surface water storage in the Ganges–Brahmaputra River Basin, *Journal of Hydrology: Regional Studies*.

Pedinotti, V., A. Boone, B. Decharme, J. F. Crétaux, N. Mognard, G. Panthou, F. Papa, and B. A. Tanimoun (2012), Evaluation of the ISBA-TRIP continental hydrologic system over the Niger basin using in situ and satellite derived datasets, *Hydrol. Earth Syst. Sci.*, *16*(6), 1745–1773, doi:10.5194/hess-16-1745-2012.

Prigent, C., E. Matthews, F. Aires, and W. B. Rossow (2001), Remote sensing of global wetland dynamics with multiple satellite data sets, *Geophys. Res. Lett.*, *28*(24), 4631–4634, doi:10.1029/2001GL013263.

Prigent, C., F. Papa, F. Aires, W. B. Rossow, and E. Matthews (2007), Global inundation dynamics inferred from multiple satellite observations, 1993–2000, *J. Geophys. Res.*, *112*(D12), D12107, doi:10.1029/2006JD007847.

Prigent, C., F. Papa, F. Aires, C. Jimenez, W. B. Rossow, and E. Matthews (2012), Changes in land surface water dynamics since the 1990s and relation to population pressure: LAND SURFACE WATER DYNAMICS, *Geophysical Research Letters*, *39*(8), n/a-n/a, doi:10.1029/2012GL051276.

Prigent, C., D. P. Lettenmaier, F. Aires, and F. Papa (2016), Toward a high-resolution monitoring of continental surface water extent and dynamics, at global scale: from GIEMS (Global Inundation Extent from Multi-Satellites) to SWOT (Surface Water Ocean Topography), *Surveys in Geophysics*, *37*(2), 339–355.

Ramillien, G., F. Frappart, A. Cazenave, and A. Güntner (2005), Time variations of land water storage from an inversion of 2 years of GRACE geoids, *Earth and Planetary Science Letters*, *235*(1–2), 283–301, doi:10.1016/j.epsl.2005.04.005.

Reason, C. J. C. (2002), Sensitivity of the southern African circulation to dipole sea-surface temperature patterns in the south Indian Ocean, *International Journal of Climatology*, *22*(4), 377–393.

Ringeval, B., N. de Noblet-Ducoudré, P. Ciais, P. Bousquet, C. Prigent, F. Papa, and W. B. Rossow (2010), An attempt to quantify the impact of changes in wetland extent on methane emissions on the seasonal and interannual time scales: WETLAND EXTENT'S CHANGES AND CH $_4$ EMISSIONS, *Global Biogeochemical Cycles*, *24*(2), n/a-n/a, doi:10.1029/2008GB003354.

Ringeval, B. et al. (2012), Modelling sub-grid wetland in the ORCHIDEE global land surface model: evaluation against river discharges and remotely sensed data, *Geosci. Model Dev.*, *5*(4), 941–962, doi:10.5194/gmd-5-941-2012.

Rodier, J. (1983), Hydrology of humid tropical regions,

Rosenqvist, \AA, and C. M. Birkett (2002), Evaluation of JERS-1 SAR mosaics for hydrological applications in the Congo river basin, *International Journal of Remote Sensing*, *23*(7), 1283–1302.

Saji, N. H., B. N. Goswami, P. N. Vinayachandran, and T. Yamagata (1999), A dipole mode in the tropical Indian Ocean, *Nature*, *401*(6751), 360–363.

Samba, G., and D. Nganga (2012), Rainfall variability in Congo-Brazzaville: 1932–2007, *International Journal of Climatology*, *32*(6), 854–873.

Samba, G., D. Nganga, and M. Mpounza (2008), Rainfall and temperature variations over Congo-Brazzaville between 1950 and 1998, *Theoretical and Applied Climatology*, *91*(1), 85–97.

Santos Da Silva, J., S. Calmant, F. Seyler, O. C. Rotunno Filho, G. Cochonneau, and W. J. Mansur (2010), Water levels in the Amazon basin derived from the ERS 2 and ENVISAT radar altimetry missions, *Remote Sensing of Environment*, *114*(10), 2160–2181, doi:10.1016/j.rse.2010.04.020.

Spigel, R. H., and G. W. Coulter (1996), Comparison of hydrology and physical limnology of the East African great lakes: Tanganyika, Malawi, Victoria, Kivu and Turkana (with reference to some North American Great Lakes), *The limnology, climatology and paleoclimatology of the East African lakes*, 103–139.

Tapley, B. D., S. Bettadpur, M. Watkins, and C. Reigber (2004), The gravity recovery and climate experiment: Mission overview and early results, *Geophys. Res. Lett.*, *31*(9), L09607, doi:10.1029/2004GL019920.

Tshimanga, R. M., and D. A. Hughes (2012), Climate change and impacts on the hydrology of the Congo Basin: The case of the northern sub-basins of the Oubangui and Sangha Rivers, *Physics and Chemistry of the Earth, Parts A/B/C*, *50–52*, 72–83, doi:10.1016/j.pce.2012.08.002.

Tshimanga, R. M., D. A. Hughes, and E. Kapangaziwiri (2011), Initial calibration of a semi-distributed rainfall runoff model for the Congo River basin, *Physics and Chemistry of the Earth, Parts A/B/C*, *36*(14), 761–774.

Ummenhofer, C. C., M. H. England, P. C. McIntosh, G. A. Meyers, M. J. Pook, J. S. Risbey, A. S. Gupta, and A. S. Taschetto (2009), What causes southeast Australia's worst droughts?, *Geophysical Research Letters*, *36*(4).

VALS Tool (2009), Virtual ALtimetry Station. Version 0.5.7.,

Verhegghen, A., P. Mayaux, C. De Wasseige, and P. Defourny (2012), Mapping Congo Basin vegetation types from 300 m and 1 km multi-sensor time series for carbon stocks and forest areas estimation, *Biogeosciences*, *9*(12), 5061.

Wahr, J., M. Molenaar, and F. Bryan (1998), Time variability of the Earth's gravity field: Hydrological and oceanic effects and their possible detection using GRACE, *Journal of Geophysical Research: Solid Earth*, *103*(B12), 30205–30229.

Watkins, M. M., D. N. Wiese, D.-N. Yuan, C. Boening, and F. W. Landerer (2015), Improved methods for observing Earth's time variable mass distribution with GRACE using spherical cap mascons, *Journal of Geophysical Research: Solid Earth*, *120*(4), 2648–2671.

Wehr, T., and E. Attema (2001), Geophysical validation of ENVISAT data products, *Advances in Space Research*, *28*(1), 83–91.

Wiese, D. N. (2015), GRACE MASCON Ocean and Hydrology Equivalent Water Heights JPL RL05M.1, , doi:10.5067/TEMSC-OCL05.

Wiese, D. N., F. W. Landerer, and M. M. Watkins (2016), Quantifying and reducing leakage errors in the JPL RL05M GRACE mascon solution, *Water Resources Research*, *52*(9), 7490–7502.

Wingham, D. J., C. G. Rapley, and Griffiths, H. (1986), New Techniques in Satellite Tracking Systems, *IGARSS '86 Symposium Digest*, *1*, 185–190.

Figure captions:

Fig. 1. The Congo River Basin: topography and the major sub-catchment areas.

Fig. 2. Location of the 350 ENVISAT radar altimeter virtual stations (black dots). Location of the in situ discharge stations (Brazzaville, Bangui and Ouesso) displayed with red triangles. Lakes are: 1. Tumba, 2. Mai-Ndombe, 3. Kivu, 4. Tanganyika, 5. Mweru and 6. Bangweulu. The locations of the four lakes using in the study are displayed with diamonds (Mai-Ndombe, Mweru, Tangkanyika and Bangweulu). Countries are AO: Angola; BU: Burundi; CT: Central African Republic; DC: Democratic Republic of the Congo; RC: Republic of the Congo; RW: Rwanda; SS: South Sudan; TZ: Tanzania; UG: Uganda; ZA: Zambia;

Fig. 3. Inundation extent from GIEMS over the Congo basin. Spatial distribution of the (a) monthly mean and (b) monthly maximum surface water extent averaged over 1993–2007, for each 773 km^2 pixel.

Fig. 4. Surface water extent seasonal variations (SWE, black) and rainfall average (blue) over 1993–2007 by sub-basins. The shaded areas depict the standard deviations around the SWE and rainfall average.

Fig. 5. Comparison of annual and interannual monthly mean surface water extent anomalies (SWE, black) and in-situ monthly mean discharge anomalies (Discharge, blue) at Brazzaville, Bangui, and Ouesso locations.

Fig. 6. Comparison of annual and interannual monthly mean surface water extent anomalies (SWE, black) and altimetry monthly mean water height anomalies (Height, blue) of Mweru, Bangweulu, and Mai-Ndombe lakes.

Fig. 7. Interannual monthly mean surface water extent (SWE) anomalies by sub-basins over 1993–2007.

Fig. 8. Seasonal evolution of the surface water heights (SWH) in meters.

Fig. 9. Maximum annual surface water storage (SWS) amplitudes in km^3 over 2003 to 2007.

Fig. 10. Percentage of surface water storage (SWS) variations per year over 2003 to 2007.

Fig. 11. Anomalies of surface water storage (SWS, black line), the GRACE-derived terrestrial water storage (TWS, blue line) and the resulting sub-surface water storage (Sub-SWS, red line) for the entire Congo River Basin and for the sub-basins.

Fig.1

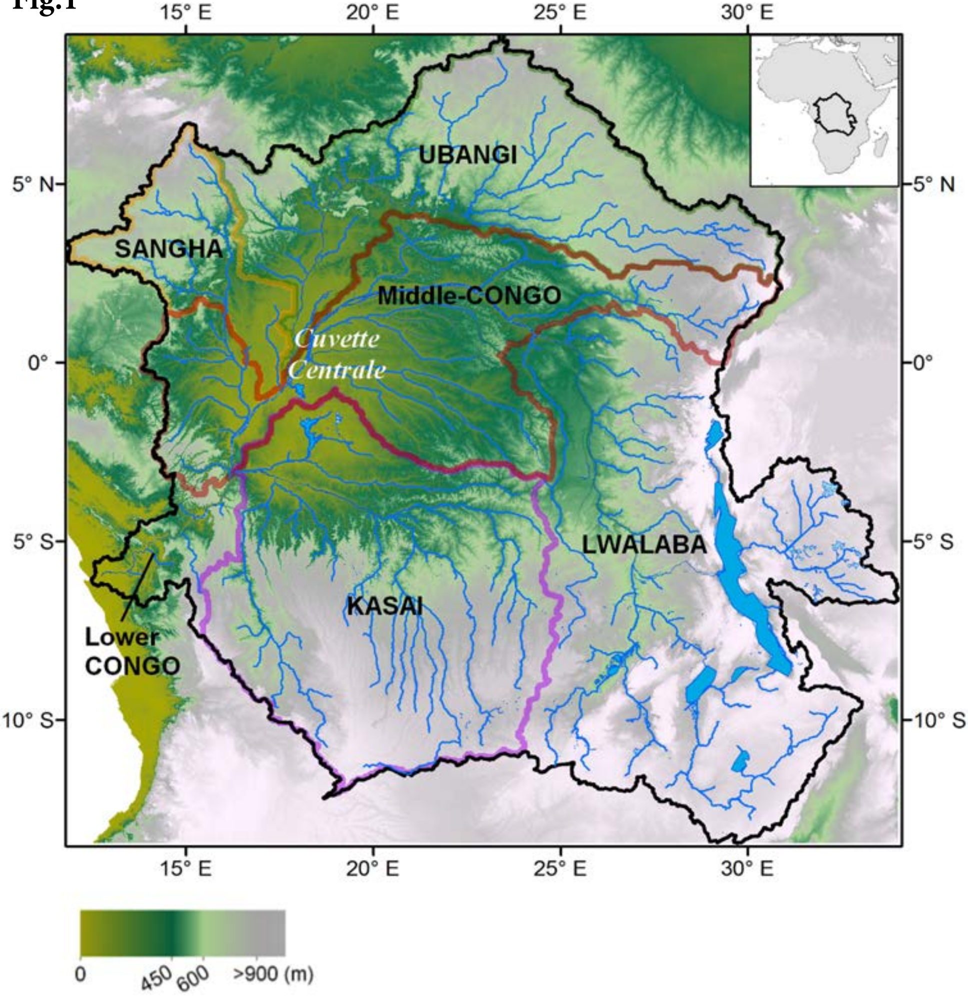

15° E
20° E
25° E
30° E
5° N
0°
5° S
10° S
UBANGI
SANGHA
Middle-CONGO
Cuvette
Centrale
LWALABA
KASAI
Lower
CONGO
0
450
600
>900 (m)

Fig.2

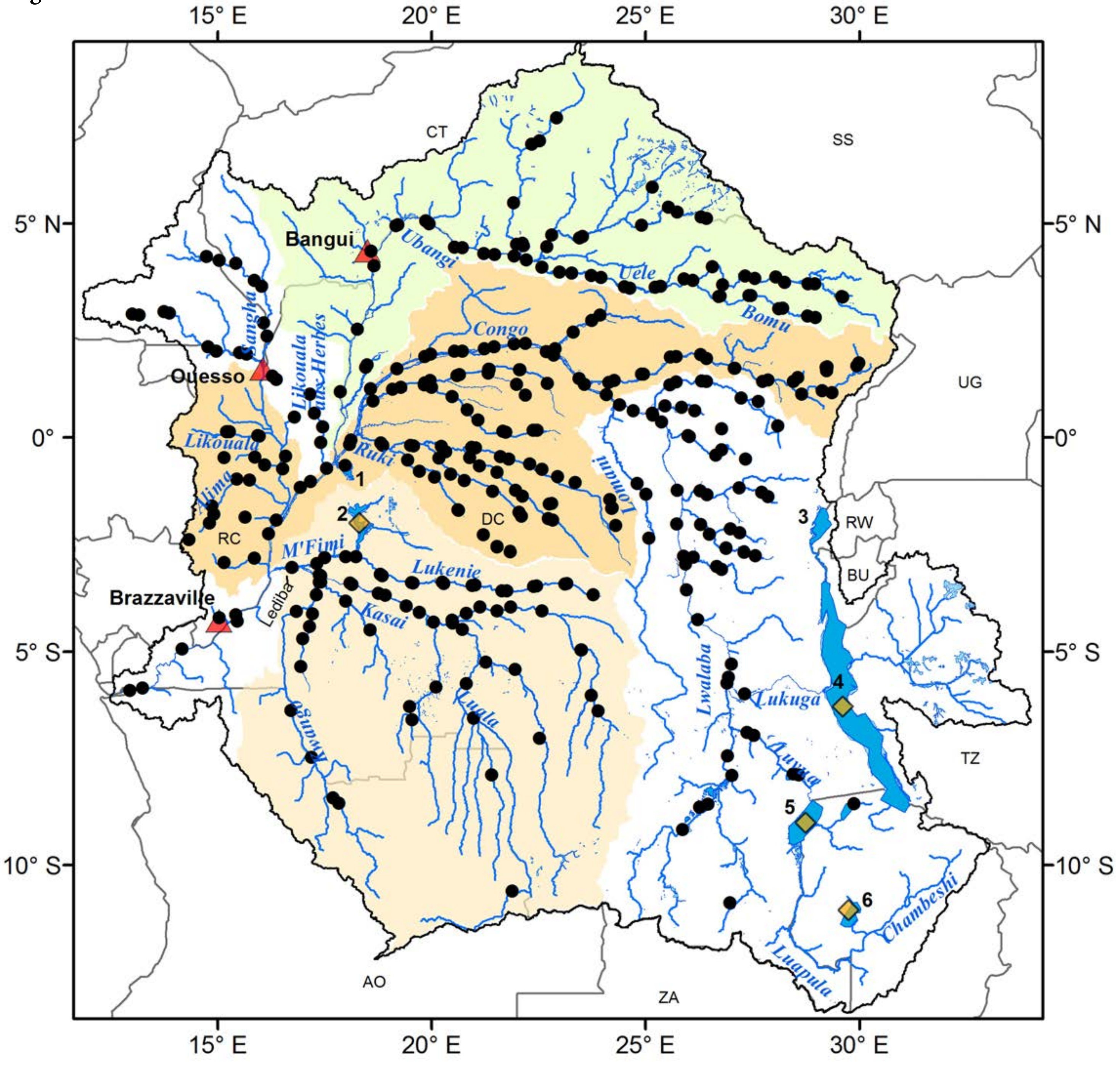
15° E
20° E
25° E
30° E
5° N
0°
5° S
10° S
CT
SS
UG
RW
BU
TZ
ZA
AO
RC
DC
Bangui
Ouesso
Brazzaville
Ubangi
Uele
Bomu
Congo
Sangha
Likouala
Likouala aux Herbes
Alima
Ruki
Lomami
M'Fimi
Lukenie
Kasai
Lediba
Kwango
Luala
Lwalaba
Lukuga
Luvua
Luapula
Chambeshi
1
2
3
4
5
6

Fig.3

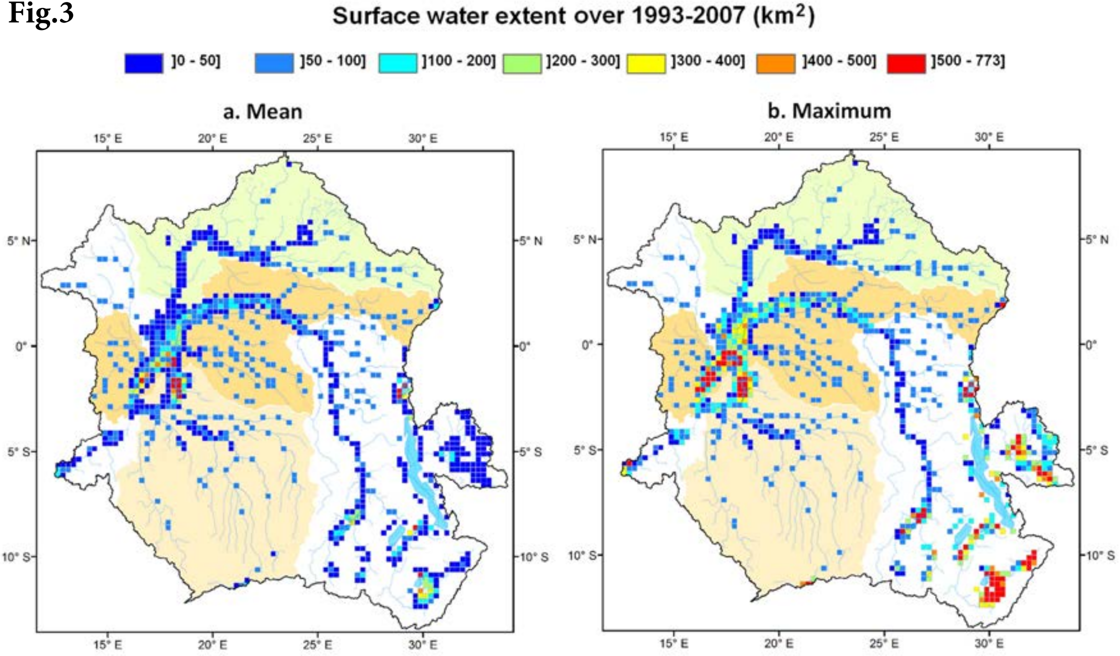
Surface water extent over 1993-2007 (km^2)
]0 - 50]
]50 - 100]
]100 - 200]
]200 - 300]
]300 - 400]
]400 - 500]
]500 - 773]
a. Mean
b. Maximum
15° E
20° E
25° E
30° E
5° N
0°
5° S
10° S

Fig.4

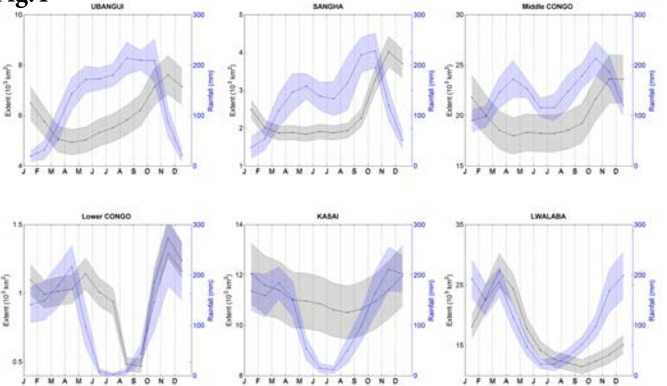
UBANGUI
SANGHA
Middle CONGO
Lower CONGO
KASAI
LWALABA
Extent (10^3 km^2)
Rainfall (mm)
J F M A M J J A S O N D

Fig.5

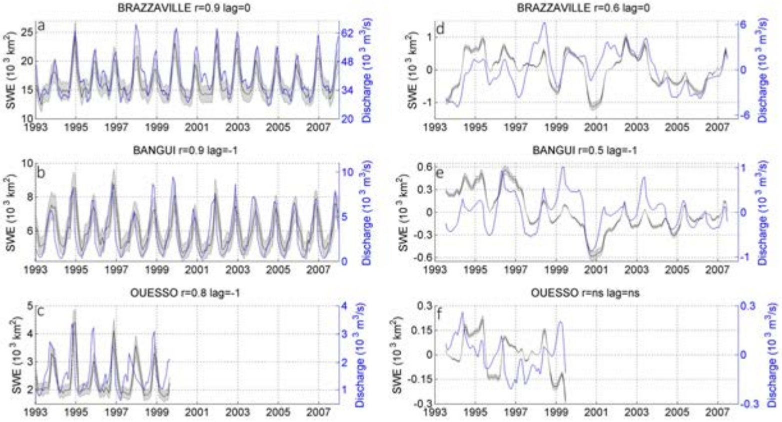
BRAZZAVILLE r=0.9 lag=0
a
SWE (10^3 km^2)
Discharge (10^3 m^3/s)
BANGUI r=0.9 lag=-1
b
OUESSO r=0.8 lag=-1
c
BRAZZAVILLE r=0.6 lag=0
d
BANGUI r=0.5 lag=-1
e
OUESSO r=ns lag=ns
f
1993 1995 1997 1999 2001 2003 2005 2007

Fig.6

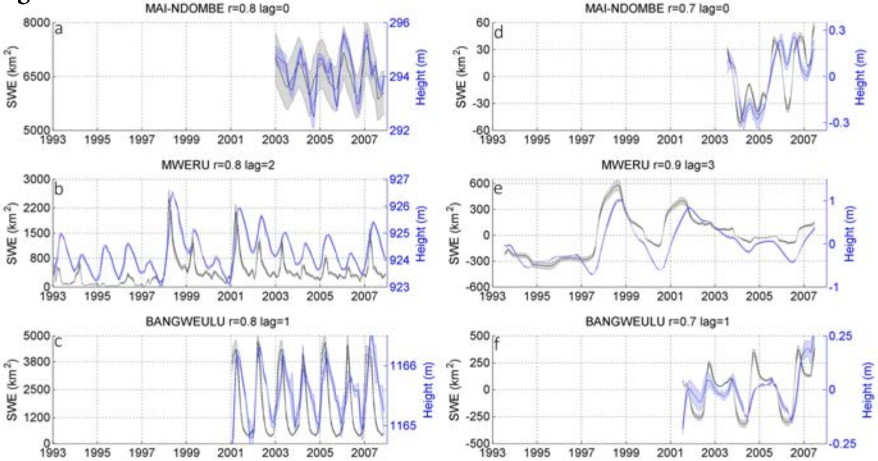

MAI-NDOMBE r=0.8 lag=0
a
SWE (km²)
Height (m)
MWERU r=0.8 lag=2
b
BANGWEULU r=0.8 lag=1
c
MAI-NDOMBE r=0.7 lag=0
d
MWERU r=0.9 lag=3
e
BANGWEULU r=0.7 lag=1
f
1993 1995 1997 1999 2001 2003 2005 2007

Fig.7

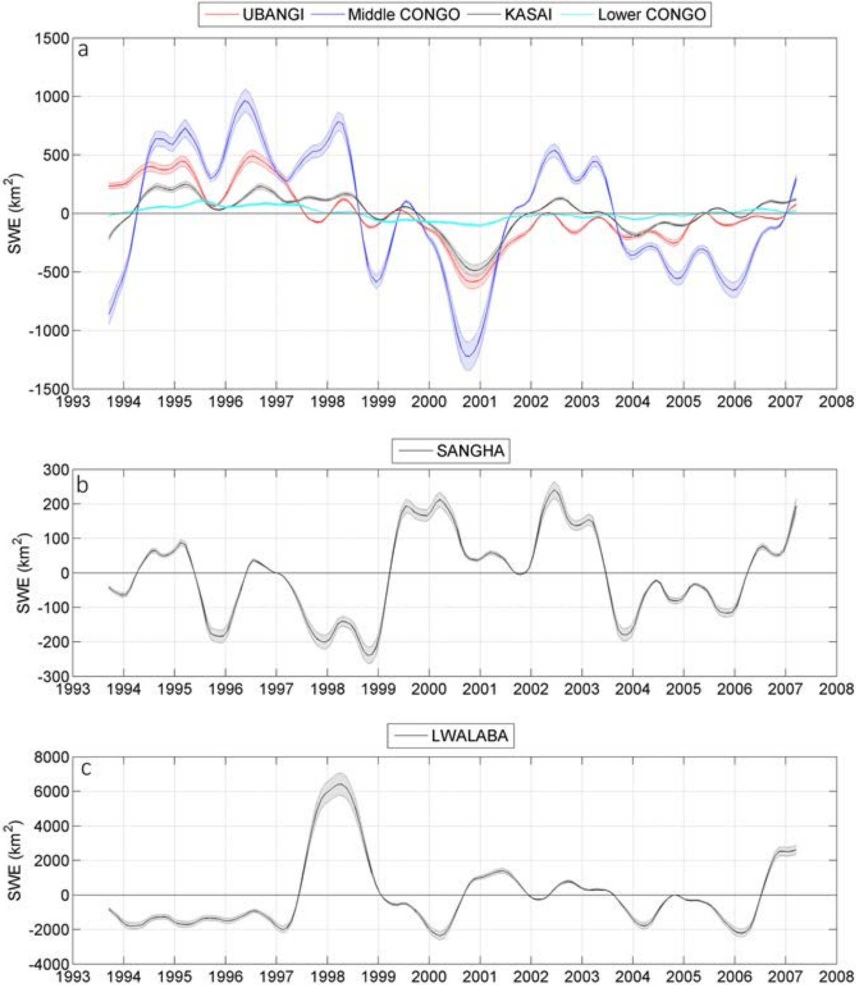

UBANGI
Middle CONGO
KASAI
Lower CONGO
a
SWE (km^2)
1500
1000
500
0
-500
-1000
-1500
1993
1994
1995
1996
1997
1998
1999
2000
2001
2002
2003
2004
2005
2006
2007
2008
SANGHA
b
300
200
100
0
-100
-200
-300
LWALABA
c
8000
6000
4000
2000
0
-2000
-4000

Fig.8

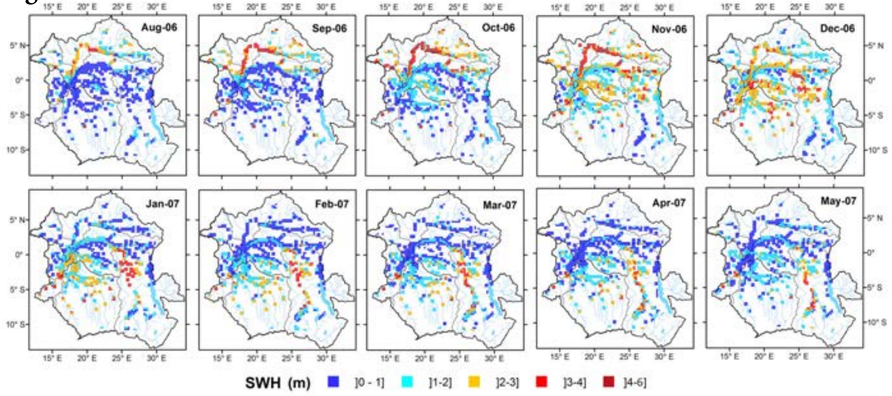
Aug-06
Sep-06
Oct-06
Nov-06
Dec-06
Jan-07
Feb-07
Mar-07
Apr-07
May-07
15° E
20° E
25° E
30° E
5° N
0°
5° S
10° S
SWH (m)
]0 - 1]
]1-2]
]2-3]
]3-4]
]4-6]

Fig.9

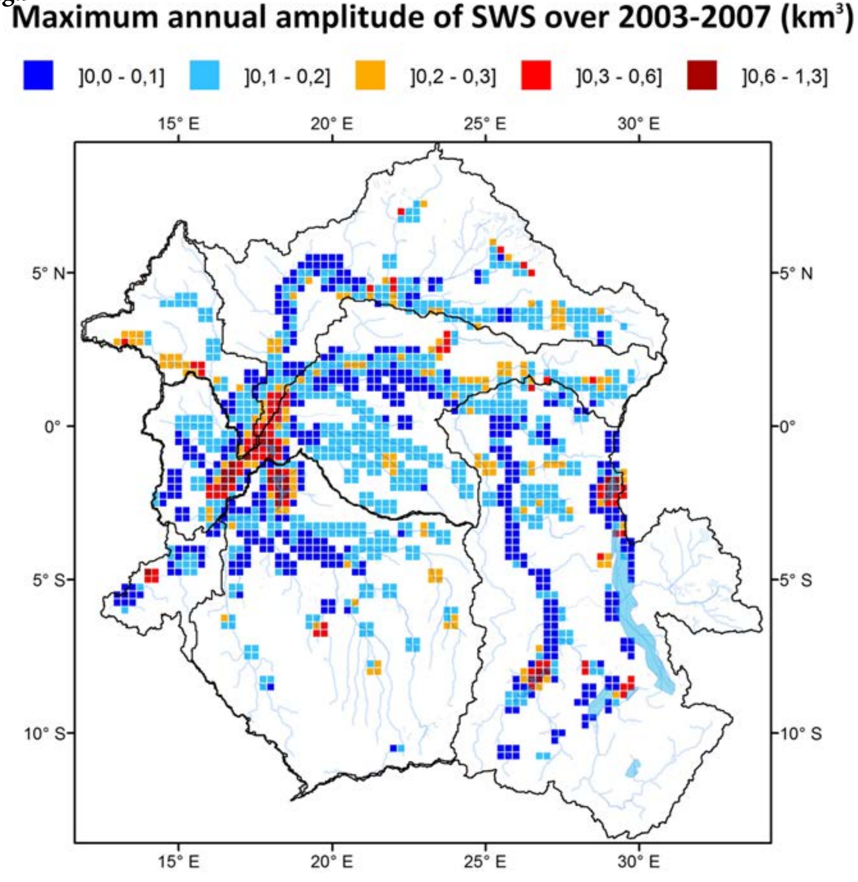
Maximum annual amplitude of SWS over 2003-2007 (km³)
]0,0 - 0,1]
]0,1 - 0,2]
]0,2 - 0,3]
]0,3 - 0,6]
]0,6 - 1,3]
15° E
20° E
25° E
30° E
5° N
0°
5° S
10° S

Fig.10

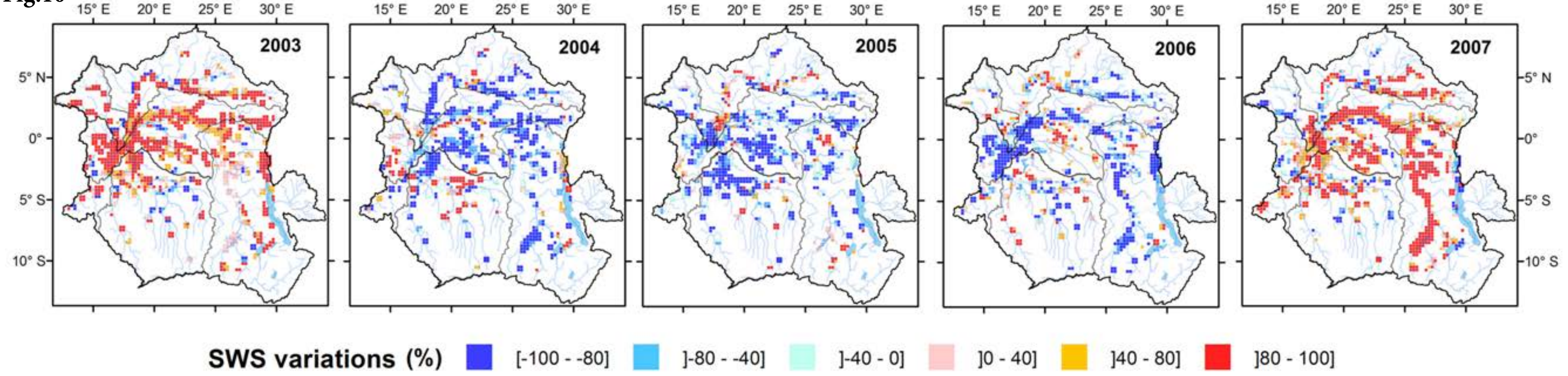

2003
2004
2005
2006
2007
15° E
20° E
25° E
30° E
5° N
0°
5° S
10° S
SWS variations (%)
[-100 - -80]
]-80 - -40]
]-40 - 0]
]0 - 40]
]40 - 80]
]80 - 100]

Fig.11

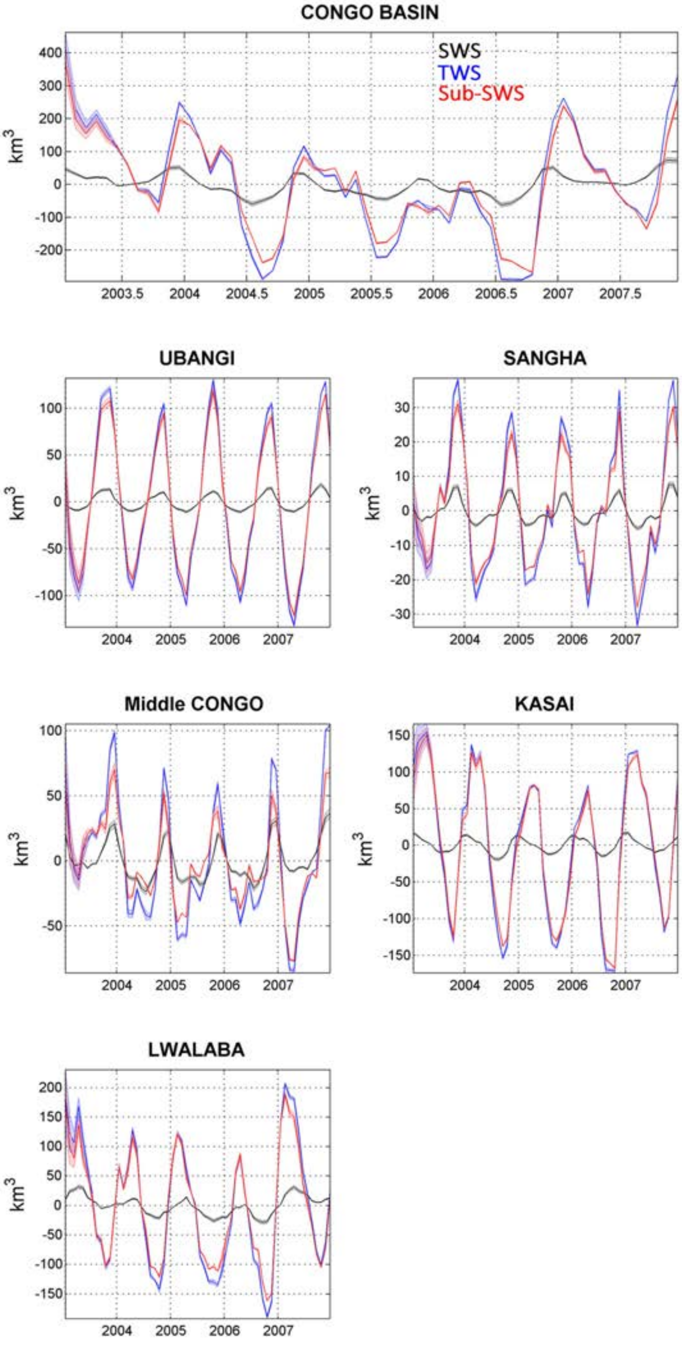
CONGO BASIN
SWS
TWS
Sub-SWS
km3
UBANGI
SANGHA
Middle CONGO
KASAI
LWALABA